

TWO SCENARIOS OF MASS EXCHANGE IN CLOSE BINARY SYSTEMS CONSISTING OF THE LOW MASS PRE-MAIN SEQUENCE STARS

F. V. Sirotkin

Astronomical observatory, Odessa National University

ABSTRACT. In this paper, we present the results of smoothed particle hydrodynamic (SPH) simulations of mass transfer in close binary systems consisting of the low mass pre-main sequence stars. Two scenarios of mass exchange in such systems are possible. If the more massive component is closer to fill its Roche lobe than the less massive, then the binary system merges as a result of the mass exchange. The binary system can survive only in the case if the less massive component is closer to fill its Roche lobe to the beginning of a mass exchange.

Key words: computational fluid dynamics, close binary system, preMS star, mass exchange, component merging.

1. Introduction

The majority of binary systems properties are gained on the pre-main sequence stage (preMS) of their evolution. Among these properties: a wide range of the mass ratios and eccentricities in the long periodic systems. One of the possible mechanisms to acquire observable properties of zero age main sequence (ZAMS) binary stars is the mass exchange on preMS evolution stage. The very important question is an explanation of the ZAMS binary stars distribution upon their mass ratio and orbital separation.

We will show, that as a result of mass exchange in preMS binary systems either merging of their components occurs, or mass exchange in a dynamic time scale results in an increase of the orbital separation and decrease of the components mass ratio.

2. Choice of initial parameters

We consider systems with the low mass components (masses between $0.5M_{\odot}$ and $1M_{\odot}$) and effective radii of the components appropriate to the time moment, when the components are near the “birthline” (Stahler, 1988) (see Fig. 1). The “birthline” is the moment when the star has lost its envelope of infalling gas and dust.

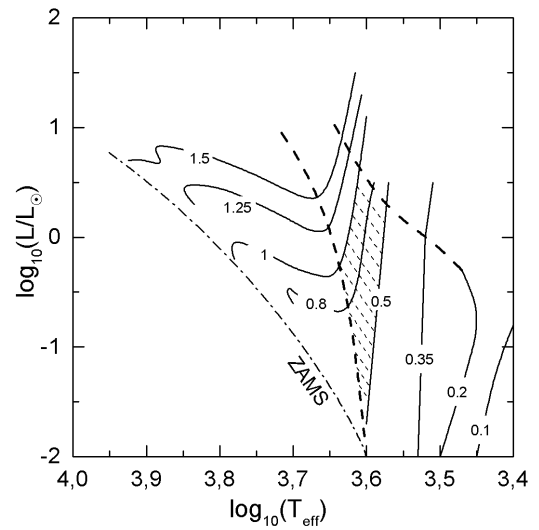


Figure 1: The theoretical pre-main-sequence tracks of Iben (1965) and Grossman and Graboske (1971), with appropriate masses (in solar units) labelled. The top dotted curve is the “birthline” (Stahler, 1988). In area between the upper and bottom dotted curves, preMS star is fully convective.

Let us designate this moment of time as t_B . At the moment t_B star of a given mass is descending a nearly vertical path. Along vertical part of the evolutionary track, the stars are fully convective, and their radii change according to this law

$$\left(\frac{R_{\odot}}{R}\right)^3 - \left(\frac{R_{\odot}}{R_B}\right)^3 = \frac{t - t_B}{t_K}, \quad (1)$$

where R_B is stellar radius at the moment of time t_B (initial radius), t - time, t_K - Kelvin-Helmholtz time:

$$t_K \sim \frac{3}{4} \frac{GM^2}{LR}.$$

As demonstrated by Stahler (1988), radius R_B depends only upon the value assumed for accretion rate and deuterium abundance (see Fig. 2), which define

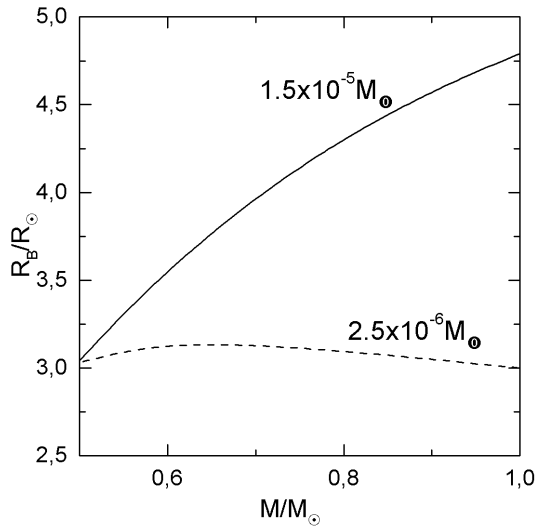


Figure 2: Mass-radius relations for the preMS stars (Stahler, 1983) located on the “birthline”. Appropriate accretion rates are labelled. Deuterium to hydrogen ratio is $[D/H] = 2.5 \cdot 10^{-3}$

the energy sources of a protostar: heating through the infalling matter and deuterium burning.

Comparison between location of the theoretical “birthline” in the Hertzsprung-Russell diagram and the region where T Tauri stars are observed has allowed to Stahler (1983) to choose for an accretion rate $\dot{M} = 10^{-5} M_{\odot} \text{ yr}^{-1}$ and deuterium abundance value $[D/H] = 2.5 \cdot 10^{-5}$. The mass-radius dependence for preMs stars with masses in the range from $0.575 M_{\odot}$ to $1.175 M_{\odot}$ on the “birthline” can be approximated by the following formula:

$$\frac{R}{R_{\odot}} = 12.6 \frac{M}{M_{\odot}} - 8.7 \left(\frac{M}{M_{\odot}} \right)^2 + 2.3 \left(\frac{M}{M_{\odot}} \right)^3 - 1.4 \quad (2)$$

The applicability of the dependencies found from observations of the single preMS stars to the binary systems depends upon the accepted hypothesis of the binary system formation. If one to assumes that the binary system was formed through fragmentation of the protostellar cloud during its dynamical collapse, it is necessary to take into account effects connected with closeness of components, and these dependencies are probably not applicable to the short periodic systems. If one assumes, that the components of the binary system were formed independently, and binary system was formed as a result of collision, then these dependencies can be applicable.

The probability of a binary system components to merge grows with degree of the filling by components of their Roche lobes. The Eq. (1) shows, that stellar radii rapidly decrease, and the probability of a binary system to merge should be much higher for the stars situated

at the beginning of the preMS stage (i.e. occupying the region closer to the “birthline”).

The orbital separation at which the components are close to fill their Roche lobes in the chosen range of the component masses is $12 R_{\odot}$. Thus we consider here the systems for which the probability of the component merging is very high.

3. Method

In the case of polytropic equation of a state:

$$P = K \rho^{\gamma}, \quad (3)$$

where γ is the ratio of specific heats (in present calculations $\gamma = 5/3$), K is the entropy function, the equation of motion of a compressible fluid can be written in the form:

$$\frac{\partial \rho}{\partial t} + \nabla \cdot (\rho \vec{v}) = 0, \quad (4)$$

$$\rho \frac{\partial K}{\partial t} + \rho (\vec{v} \cdot \nabla) K = - \frac{\gamma - 1}{\rho^{\gamma}} \mathfrak{S}. \quad (5)$$

$$\frac{\partial \vec{v}}{\partial t} + (\vec{v} \cdot \nabla) \vec{v} = - \frac{1}{\rho} \nabla P - \vec{F}, \quad (6)$$

where ρ is the density, \vec{v} the velocity, P pressure, and the \mathfrak{S} the energy loss function which comprises all nonadiabatic sources and sinks of energy.

In SPH (Lucy, 1977; Gingold & Monaghan, 1977), these equations of motion are solved using Lagrangian formulation in which the gas is partitioned into fluid elements. A subset of these fluid elements are selected and represented by particles. In SPH these subset is chosen so that the particle mass density is proportional to the fluid density, ρ . This means that ρ can be estimated from the local density of particles at later times if the system is updated according to the equations of hydrodynamics.

Since the number of particles is finite, it is necessary to introduce a “smoothing” procedure to interpolate between them to represent the fields as continuous quantities. If each particle has a mass m_j then the SPH-smoothed density is given by

$$\rho(\vec{r}) = \sum_{i=1}^N m_i W(|\vec{r} - \vec{r}_i|, h), \quad (7)$$

where h_i is the smoothing length, and $W(r, h)$ is the smoothing kernel which satisfies the following conditions:

$$\int W(r - r', h) dr' = 1, \quad (8)$$

$$\lim_{h \rightarrow 0} W(r - r', h) = \delta(r - r'). \quad (9)$$

The calculations presented here were performed using the Gaussian kernel

$$W(r, h) = \frac{\exp(-r^2/h^2)}{\pi^{3/2} h^3}, \quad (10)$$

In the implementation used here the components of a binary system have their own fixed smoothing length. The primary component is described by N_p particles with smoothing length h_p and mass $m_p = M_1/N_p$. The secondary component is described by N_s particles with smoothing length h_s and mass $m_s = M_2/N_s$, $N_s = N - N_p$, where N is the total number of particles. For this case the SPH form of the equation (7)

$$i s \rho_i = \sum_{j=1}^N m_j W_{ij}, \quad (11)$$

$$W_{ij} = W(r_{ij}, h_i)/2 + W(r_{ij}, h_j)/2 \quad (12)$$

where ρ_i is the smoothing density at the point \vec{r}_i , and $r_{ij} = |\vec{r}_i - \vec{r}_j|$.

SPH form of the equation (4) is the following

$$\begin{aligned} \frac{d\vec{v}_i}{dt} = & - \sum_{j=1}^N m_j \left(\frac{P_i}{\rho_i^2} + \frac{P_j}{\rho_j^2} \right) \cdot \nabla_i W_{ij} - \\ & - G \sum_{j=1}^N \frac{M(r_{ij})}{r_{ij}^2} \frac{\vec{r}_{ij}}{r_{ij}} + \vec{a}_i^{visc} \quad (13) \\ M(r_{ij}) = & 4\pi m_i \int_0^{r_{ij}} r^2 W(r, h) dr, \end{aligned}$$

where G is the Newtonian gravitation constant. The second term in equation (13) is the gravitational forces, \vec{a}_i^{visc} is the viscous forces. The standard artificial viscosity is employed (Monaghan, 1992):

$$\vec{a}_i^{visc} = \sum_{j=1}^N m_j \Pi_{ij} \nabla_i W_{ij}, \quad (14)$$

where

$$\Pi_{ij} = \frac{-\alpha \mu_{ij} c_{ij} - \beta \mu_{ij}^2}{\rho_{ij}} \quad (15)$$

$$\mu_{ij} = \begin{cases} \frac{\vec{v}_{ij} \cdot \vec{r}_{ij}}{h(r_{ij}^2/h^2 + \eta^2)}, & \vec{v}_{ij} \cdot \vec{r}_{ij} < 0 \\ 0, & \vec{v}_{ij} \cdot \vec{r}_{ij} \geq 0 \end{cases} \quad (16)$$

and $\vec{v}_{ij} = \vec{v}_i - \vec{v}_j$, $\vec{r}_{ij} = \vec{r}_i - \vec{r}_j$, $c_{ij} = c_i - c_j$ is the average speed of sound of particles i and j , $h_{ij} = (h_i + h_j)/2$, $\rho_{ij} = (\rho_i + \rho_j)/2$. The numerical simulation is performed with constant $\alpha = 0.5$, $\beta = 1$, $\eta = 0.001$.

Ignoring any sources of entropy other than artificial viscosity, the smoothed equation (5) for the entropy function K is

$$\frac{dK_i}{dt} = \frac{\gamma - 1}{2\rho_i^{\gamma-1}} \sum_{j=1}^N \Pi_{ij} m_j \vec{v}_{ij} \cdot \nabla_i W_{ij} \quad (17)$$

The solution of the equations (11), (13), (17) is determined by a choice of the initial conditions. We establish the initial conditions in such way that at the

initial moment of time the binary components are in the state near the stationary equilibrium. The construction of such initial conditions can be divided into three steps:

- The first step is the construction of internal structure of each component as a star in the state of hydrostatic equilibrium.
- The second step is to take into account rotation of each component and tidal forces operating between them.
- The last step is coordinate transformation and establishing of the initial speed of particles.

At the first step the models were constructed by laying particles down randomly and then solving equation (13) in the presence of frictional dumping to achieve a stationary equilibrium (Gingold and Monaghan, 1977).

At the second stage we take into account rotation and tidal forces. For each binary component the tidal forces were estimated considering another companion as a point mass.

At the last step we make transformation of coordinates. For the primary component this transformation of coordinates can be written as follows':

$$\vec{r}_i = \vec{r}_i + \vec{r}_{cm1}, \quad \vec{v}_i = \vec{\Omega} \times \vec{r}_i, \quad i = 1 \dots N_p, \quad (18)$$

and for the secondary one:

$$\vec{r}_i = \vec{r}_i + \vec{r}_{cm2}, \quad \vec{v}_i = \vec{\Omega} \times \vec{r}_i, \quad i = N_p + 1 \dots N, \quad (19)$$

where \vec{r}_{cm1} is the primary component's center of mass, \vec{r}_{cm2} is the secondary component's center of mass. The initial angular velocity $\vec{\Omega}$ was set in units of the Keplerian angular velocity $\vec{\Omega}_K$:

$$\vec{\Omega} = k_\Omega \vec{\Omega}_K, \quad |\vec{\Omega}_K| = \sqrt{\frac{GM}{A^3}} \quad (20)$$

where A is the orbital separation, $M = M_1 + M_2$. In close binaries, the tidal distortion of a star by its companion gives rise to a perturbation of the external gravitational field which in turn causes a secular motion of the line of the apses (Stern, 1939):

$$\frac{d\omega}{dt} = \left(\frac{R_1}{A} \right)^5 \Omega_K q k_2 15 (1 - e^2)^{-5} \left(1 + \frac{3e^2}{2} + \frac{e^4}{8} \right) \quad (21)$$

where $q = M_2/M_1$ is the mass ratio, e is the orbital eccentricity, ω is the longitude of the periastron. The apsidal-motion constant k_2 depends on the internal structure of the star and measures the extent to which mass is concentrated towards the stellar center. For the preMS stars along their vertical part of the evolutionary track the apsidal-motion constant is typically of the order of $10^{-1} - 10^{-2}$. For systems with circular orbits this means that the angular velocity higher than

the Keplerian angular velocity (i.e. $k_\Omega > 1$). To estimate parameter k_Ω one can use the following formula

$$k_\Omega = 1 + \frac{0.22q^{7.71}}{32.13q^{7.46} + \ln(1 + q^{6.48})}. \quad (22)$$

This formula is correct in case if the orbital eccentricity is zero, the primary component fill its Roche lobe, the secondary component is point mass and the ratio of specific heats γ equals to 5/3.

4. Results

Models were created by a method described above with component masses in the range from $0.575M_\odot$ to $1.175M_\odot$, with the parameter k_Ω in the range from 0.95 to 1.01. The mass of the binary system equals to $1.75M_\odot$ and the initial orbital separation equals to $12R_\odot$ for all the models. For the description of each component 3000 points were used. Models were divided into two groups.

The initial stellar radii of the models of group "B" obey the law (2). For these models

$$\frac{R_1}{R_1^e} > \frac{R_2}{R_2^e}, \quad (23)$$

where R_1^e and R_2^e are the Roche lobe equivalent radii of the primary (more massive) and secondary component, R_1 and R_2 are the equivalent radii of the primary and secondary component respectively. The Roche lobe equivalent radius is the radius of the sphere having the volume which is equal to the Roche lobe volume. The component equivalent radius is the radius of the sphere having the volume which is equal to the component volume.

The initial stellar radii of the models group "A" do not obey the law (2). For these models:

$$\frac{R_1}{R_1^e} < \frac{R_2}{R_2^e}, \quad (24)$$

and R_2/R_2^e for the group "A" is equal to R_1/R_1^e for the group "B". Stellar radii quickly decrease according to the Eq. (1). More massive stars collapse faster. Thus, there can be a situation at which less massive component of the binary system can be closer to fill its Roche lobe, than the more massive component. For all the models initial stellar radii are smaller than the corresponding Roche lobe:

$$\frac{R_1}{R_1^e} < 1, \quad \frac{R_2}{R_2^e} < 1. \quad (25)$$

Twenty models were created for each group.

Group "A". For these models the result of mass transfer depends upon initial angular velocity of the system. The range of value k_Ω , where mass transfer

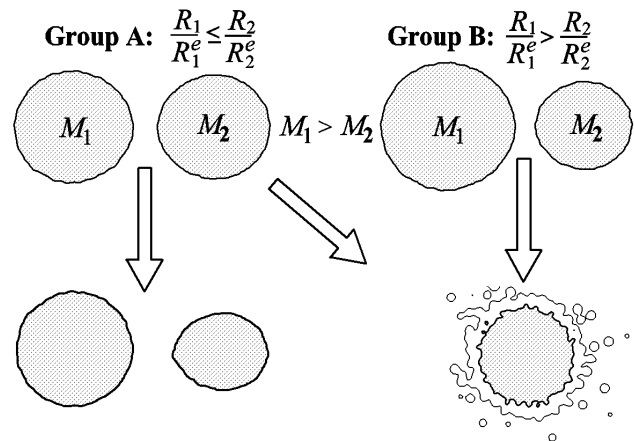


Figure 3: Flowchart of the mass transfer for the preMS close binaries. Letters "A" and "B" corresponds to the groups of the models.

exists, is narrower for the mass ratio close to unit. Let us consider this on an example of one model.

Initial density distribution for the model with initial parameters $M_1 = 1.075$, $R_1 = 4.81$, $R_1/R_1^e = 0.95$, $M_2 = 0.685$, $R_2 = 3.96$, $R_2/R_2^e = 0.97$ are presented in Fig. (4a), (4d). Initial period of this system is 3.63 days and initial mass ratio $q = M_2/M_1$ is 0.63. In the range of values of k_Ω from 0.95 to 1.005, the orbital separation decreases as a result of kinetic energy dumping on nonequilibrium tides. Less massive component begins to overflow its Roche lobe, and mass transfer begins (see Fig. (4b), (4e)) correspondently. Orbital separation increases as a result of mass transfer, and mass transfer respectively finishes. Final mass ratio and orbital separation depend upon initial parameters, but orbital separation increases and mass ratio decreases for any initial parameters for which mass transfer in this group exists. For example, in case of the value $k_\Omega = 0.97$ the final value of orbital separation is $16R_\odot$ and value of the mass ratio is 0.17. For the value $k_\Omega = 1$ the final value of orbital separation is $14.5R_\odot$ and the value of the mass ratio is 0.28 (see Fig. (4c), (4f)). The components merge which the value $k_\Omega < 0.95$.

Group "B". If the mass transfer began, the models of this group merge always. For model with initial parameters $M_1 = 1.075$, $R_1 = 4.93$, $R_1/R_1^e = 0.97$, $M_2 = 0.675$, $R_2 = 3.87$, $R_2/R_2^e = 0.95$ initial density distribution presented in Fig. (5a), (5d). This model differs from the previous one on only on the components radii. And this difference is small, but for this model if there is a mass transfer then components merge always.

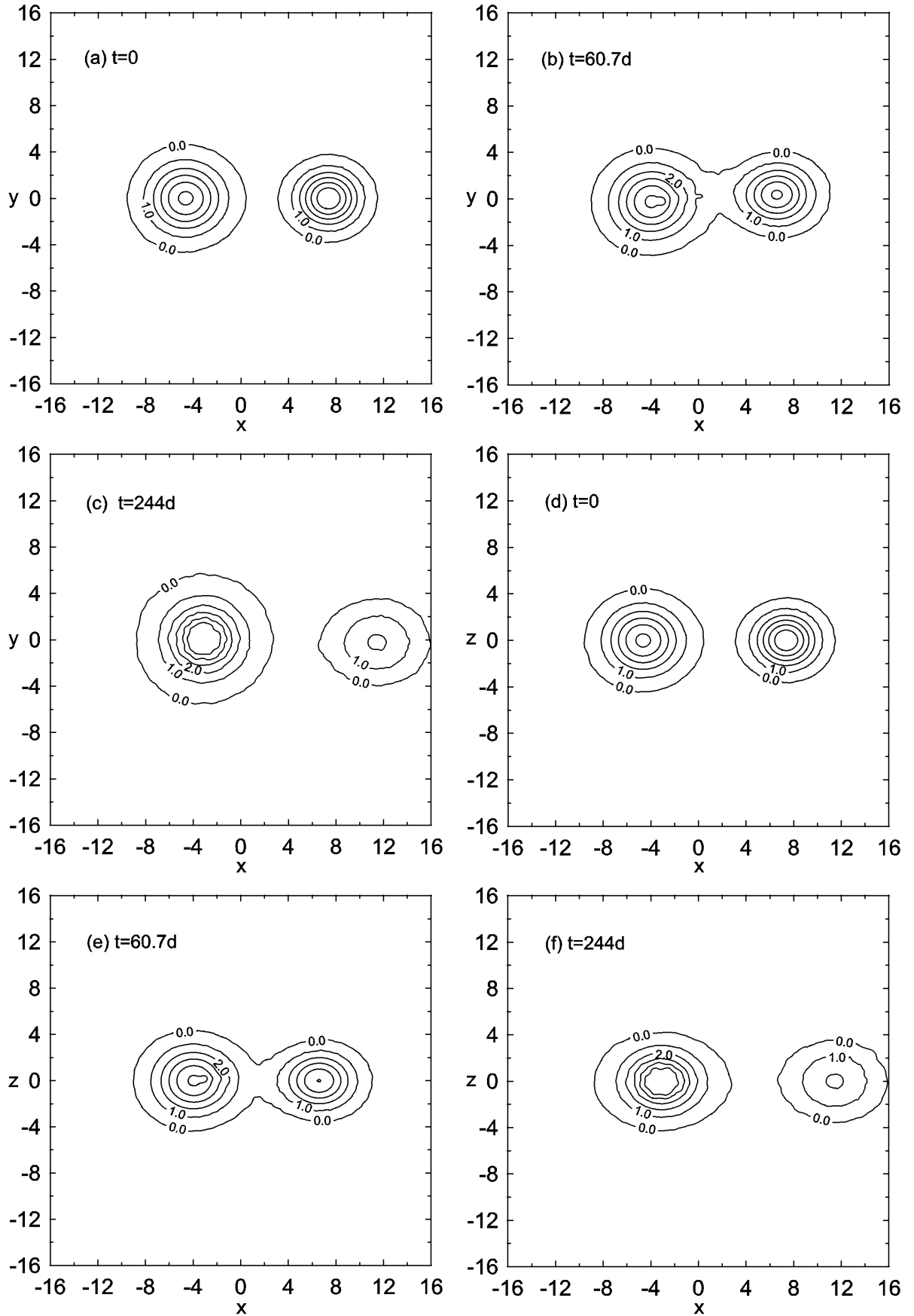


Figure 4: Model A. The density contours in the orbital plane (a,b,c), and in the XOZ plane (d,e,f) for the moments of time labeled. $M_1 = 1.075$, $R_1 = 4.81$, $R_1/R_1^e = 0.95$, $M_2 = 0.685$, $R_2 = 3.96$, $R_2/R_2^e = 0.97$, $k_\Omega = 1$, $M_2/M_1 = 0.615$. Distances are given in terms of R_\odot . Density is given in terms of $3\pi(M_1/R_1^3 + M_2/R_2^3)/8$

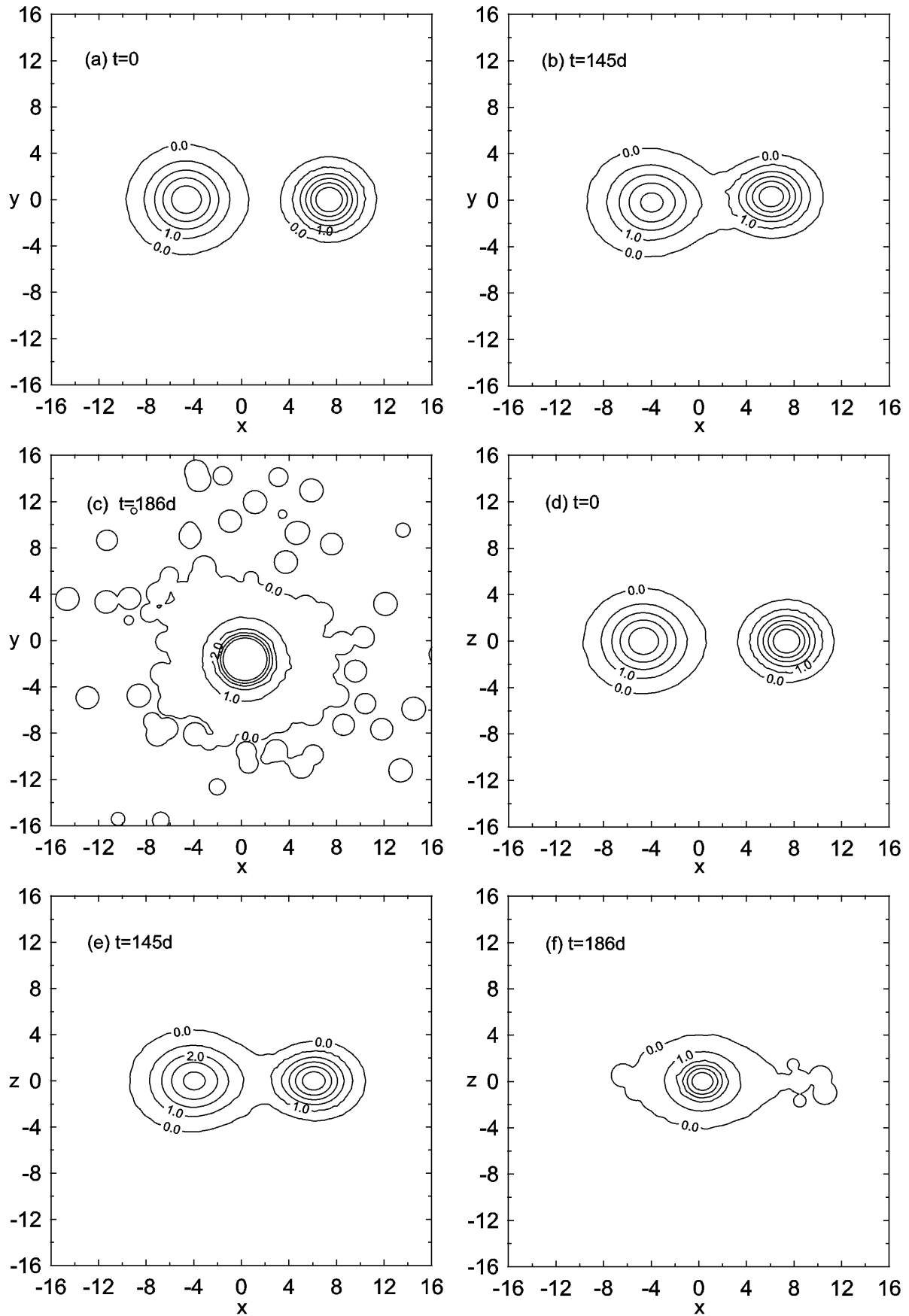


Figure 5: Model B. The density contours in the orbital plane (a,b,c), and in the XOZ plane (d,e,f) for the moments of time labeled. $M_1 = 1.075$, $R_1 = 4.93$, $R_1/R_1^e = 0.97$, $M_2 = 0.675$, $R_2 = 3.87$, $R_2/R_2^e = 0.95$, $k_\Omega = 1$, $M_2/M_1 = 0.615$. Distances are given in terms of R_\odot . Density is given in terms of $3\pi(M_1/R_1^3 + M_2/R_2^3)/8$

5. Conclusion

- In the case if the more massive component is closer to fill its Roche lobe, the components merge always.
- In the case if the less massive component closer to fill its Roche lobe, the mass transfer can occur in a dynamic time scale.
- The orbital separation increases, and the mass ratio decreases as a result of the mass transfer.
- Probability of existence of preMS close binary systems with the less massive component which closer to the filling its Roche lobe higher, than systems where the more massive component closer to fill its Roche lobe.

- The number of the preMS close binary systems should decrease for the mass ratio close to unit.

The basic conclusions are correct for other part evolutionary track, for which the assumption about fully convective stellar interior is correct.

References

- Iben I.: 1965, *Ap. J.*, **141**, 993.
Gingold R.A., Monaghan J.J.: 1977, *MNRAS*, **181**, 375-389.
Grossman A.N. and Graboske H.C.: 1971, *Ap. J.*, **164**, 475.
Lucy L.B.: 1977, *Astron. J.*, **82**, 1013.
Monaghan J.J.: 1992, *Annu. Rev. Astron. Astrophys.*, **30**, 543-74.
Stahler S.W.: 1983, *Ap. J.*, **274**, 822.
Stahler S.W.: 1988, *Ap. J.*, **332**, 804-825.
Stern T.E.: 1939, *MNRAS*, **99**, 451.